



HAL
open science

An Experimental Study on the Secondary Deformation of Boom Clay

Yongfeng Deng, Yu-Jun Cui, Anh Minh A.M. Tang, Xiang-Ling Li, Xavier
Sillen

► **To cite this version:**

Yongfeng Deng, Yu-Jun Cui, Anh Minh A.M. Tang, Xiang-Ling Li, Xavier Sillen. An Experimental Study on the Secondary Deformation of Boom Clay. *Applied Clay Science*, 2012, 59-60, pp.19-25. 10.1016/j.clay.2012.02.001 . hal-00693412

HAL Id: hal-00693412

<https://enpc.hal.science/hal-00693412>

Submitted on 2 May 2012

HAL is a multi-disciplinary open access archive for the deposit and dissemination of scientific research documents, whether they are published or not. The documents may come from teaching and research institutions in France or abroad, or from public or private research centers.

L'archive ouverte pluridisciplinaire **HAL**, est destinée au dépôt et à la diffusion de documents scientifiques de niveau recherche, publiés ou non, émanant des établissements d'enseignement et de recherche français ou étrangers, des laboratoires publics ou privés.

1 **An Experimental Study on the Secondary Deformation of Boom Clay**

2
3 **Y.F. Deng^{1,2}, Y.J. Cui², A.M. Tang², X.L. Li³, X. Sillen⁴**

- 4
5 1. Southeast University, Institute of Geotechnical Engineering, Transportation College,
6 Nanjing, China (noden@163.com)
7 2. Ecole des Ponts ParisTech, Navier/CERMES, Marne-la-Vallée, France
8 (yujun.cui@enpc.fr)
9 3. Euridice Group, c/o SCK/CEN, Mol, Belgium (xli@sckcen.be)
10 4. ONDRAF/NIRAS, Belgium (xavier.sillen@sckcen.be)

11
12
13
14
15
16
17 **Corresponding author**

18 Prof. Yu-Jun Cui

19 Ecole des Ponts ParisTech, UMR Navier/CERMES

20 6-8 av. Blaise Pascal, Cité Descartes, Champs-sur-Marne

21 F-77455 MARNE-LA-VALLEE CEDEX 2

22 France

23
24 E-mail: yujun.cui@enpc.fr

25 Tel: +33 1 64 15 35 50

26 Fax: +33 1 64 15 35 62

27 **Abstract**

28 Boom clay formation, a deposit of slightly over-consolidated marine clay that belongs to the
29 Oligocene series in the north east of Belgium, has been selected as a possible host material of
30 nuclear waste disposal. In this context, the long-term deformation behaviour of Boom clay is
31 of crucial importance in the performance assessment of the whole storage system. In this
32 study, low and high pressure oedometer tests are carried out; the e-log σ'_v (void ratio –
33 logarithm of vertical effective stress) and e-log t (void ratio – logarithm of time) curves
34 obtained are used to determine the compression index C_c^* , swelling index C_s^* and secondary
35 deformation coefficient C_α during both loading and unloading. The relationship between C_α
36 and the effective stress ratio (σ'_v/σ'_c , vertical effective stress to pre-consolidation stress) is
37 analysed, and it is observed that C_α increases linearly with $\log \sigma'_v/\sigma'_c$. Examination of the
38 ratio of C_α/C_c^* for various soils shows that the secondary deformation behaviour of Boom
39 clay is similar to that of shale and mudstone. The relation between C_α and C_c^* is linear; but
40 the relation between C_α and C_s^* is bi-linear. The bi-linearity observed is related to two
41 different mechanisms: the mechanically dominated rebounding and the physico-chemically
42 dominated swelling.

43

44 **Keywords:** Boom clay; oedometer test; secondary deformation behavior; mechanically
45 dominated rebounding; physico-chemically dominated swelling.

46 1. Introduction

47 Boom clay formation, a thick deposit of slightly over-consolidated marine clay has been
48 selected as a possible host material of nuclear waste disposal in Belgium. In this context, its
49 volume change behaviour, especially its secondary deformation behaviour is essential for the
50 safety of the whole storage system, and therefore needs to be investigated in depth.

51 The consolidation of fine-grained soils has been commonly described by the primary
52 consolidation and the secondary consolidation. The former refers to the soil volume change
53 due to water pressure dissipation whereas the latter refers to the soil volume change due to the
54 evolution of soil fabric and soil-water interaction. In the past decades, many studies were
55 conducted to correlate the secondary deformation coefficient (C_α) during loading with other
56 soil characteristics. Walker (1969) showed that C_α varied with the ratio of vertical effective
57 stress (σ'_v) to the pre-consolidation pressure (σ'_c), with the largest C_α at a stress slightly
58 higher than σ'_c . This was confirmed by other studies on various soils (Brook and Mark, 2000;
59 Yilmaz and Saglamer, 2004; You, 1999; Zhu *et al.*, 2005; Shirako *et al.*, 2006; Suneel *et al.*,
60 2008; Costa and Ioannis, 2009). Walker and Raymond (1968) found that the secondary
61 deformation coefficient (C_α) during loading has a linear relationship with the compression
62 index (C_c) over the full range of stress applied. This C_α - C_c relation was further investigated by
63 many other researchers (Mesri and Castro, 1987; Mesri *et al.*, 1997; Abdullah *et al.*, 1997;
64 Al-Shamrani, 1998; Brook and Mark, 2000; You, 1999; Feng *et al.*, 2001; Tan, 2002; Mesri,
65 2004; Zhang *et al.*, 2005; Zhu *et al.*, 2005; Costa and Ioannis, 2009; Feng and Zhu, 2009;
66 Mesri and Vardhanabhuti, 2009) on various soils (intact clays, remoulded clays, clays treated
67 with lime or cement, and sands); the results confirmed the observation by Walker and
68 Raymond (1968). Mesri *et al.* (1994) defined four groups of soils according to the value of the
69 ratio C_α/C_c (Table 1). Some other correlations were also attempted between C_α/C_c (or C_α) and
70 soil physical properties such as the liquid limit w_L , plastic limit w_P and plasticity index I_p
71 (You, 1999; Suneel *et al.*, 2008).

72 Although the secondary consolidation behaviour of soils has been widely investigated,
73 there have been few studies on the stiff Boom clay, especially on the unloading path that
74 represents the situation of the soil in vicinity of excavated galleries. In the present work,
75 consolidation tests are performed in both low and high pressure oedometers on Boom clay
76 taken from the sites of Essen and Mol, Belgium. Loading and unloading are run in steps and
77 the secondary deformation coefficient C_α is determined for each step. Furthermore, the
78 relations between C_α , the effective stress ratio (σ'_v/σ'_c), compression and swelling indexes
79 (C_c^* and C_s^*) are analyzed. The main objective is to study the variations of C_α during
80 unloading and the mechanisms involved in these variations. Note that the use of high pressure
81 oedometer in this study allows studying the variation of C_α at large stress ratio σ'_v/σ'_c ,
82 indispensable for deeply located soil as Boom clay (223 m deep in Mol and about 240 m in
83 Essen). Moreover, the introduction of parameter C_c^* and C_s^* allows analysing the soil
84 compression behaviour with a non-linear loading-unloading curve. Note also that, to the
85 authors' knowledge, there have been no studies before focusing on the variations of C_α during
86 unloading.

87 2. Soil studied

88 The soil studied was taken by coring at the sites of Essen and Mol, Belgium. The location of
89 the two sites is shown in Figure 1 (De Craen *et al.*, 2006). The Essen site is situated in the
90 north east of Belgium, about 60 km far from the underground research laboratory (URL) at
91 the Mol site. After being taken from the borehole, the cores were sealed in plastic tubes
92 having ends closed and transported to the laboratory. Five soil cores of 1-m length and
93 100-mm in diameter from Essen and one soil core of 0.5-m length and 100-mm in diameter
94 from Mol were studied. The details of these cores are shown in Table 2, with the
95 corresponding depth, member, unit mass of solids (ρ_s), liquid limit (w_L), plastic limit (w_P),
96 plasticity index (I_p), water content (w_0) and void ratio (e_0). There are three cores taken from
97 the Putte member (Mol, Ess75 and Ess83) and three cores from the Terhagen members (Ess96,
98 Ess104 and Ess112). The geotechnical identification parameters of the cores from Essen are
99 similar: $\rho_s = 2.64 - 2.68$; $w_L = 62 - 78\%$; $w_P = 25 - 33\%$; $I_p = 36 - 45$. The values are also
100 close for both water content and void ratio: $w_0 = 27.2 - 29.7$, $e_0 = 0.700 - 0.785$. For the core
101 from Mol, the values of ρ_s , w_L , w_P and I_p are similar to that of the cores from Essen, but the
102 water content and void ratio are lower than the cores from Essen, showing that Boom clay
103 from Mol is denser.

104 3. Experimental techniques

105 Both low pressure (0.05 - 3.2 MPa) and high pressure (0.125 - 32MPa) oedometer tests were
106 carried out following the French standards (AFNOR 1995, 2005) on the six Boom clay cores.
107 The tests in low pressure oedometer aim at studying the loading-unloading behavior of the
108 soil near the excavation gallery, whereas the tests in high pressure oedometer aim at studying
109 the compression behavior in large stress level (far from the excavation gallery). The soil
110 samples were prepared by trimming and had 50-mm in diameter and 20-mm in height. In the
111 following, high pressure oedometer test is named Oedo1 while low pressure test is named
112 Oedo2. Note that the high pressure oedometer has the same principle as the standard low
113 pressure oedometer; the main difference is that in high pressure oedometer two amplification
114 levels were used with a ratio of 1:10 for the first level and 1:5 for the second level (see Figure
115 2). In other words, the frame of high pressure oedometer allows multiplying the applied
116 weight by 50, which leads to a maximum force of 12 tons. In the experiments, the minimum
117 and maximum applied weights are 5 N and 1280 N, leading to a minimum and maximum
118 vertical pressure of 0.125 MPa and 32 MPa respectively for a sample of 50 mm diameter.

119 The soil specimen was installed in the cell with dry porous stones. Prior to circulation of
120 the synthetic water which has the same chemistry as the in-situ pore water (Cui *et al.*, 2009)
121 in the drainage system, a confining pressure equal to the estimated in situ stress was applied.
122 This prevents the soil swelling during re-saturation which may modify the soil microstructure
123 and as a result the soil mechanical properties (Delage *et al.*, 2007).

124 The in situ stress of the soil was estimated using Eq. 1:

$$125 \quad \sigma'_{v0} = \gamma h - u_0 \quad (1)$$

126 where σ'_{v0} is the in situ effective vertical stress; γ is the mean unit weight of the soil above the
127 depth considered, taken equal to 20 kN/m³ following the data of De Craen *et al.* (2006); h is

128 the depth of the soil core (see Table 2); u_0 is the in situ pore pressure estimated from the
129 ground water level that is assumed to be at the ground surface. The σ'_{v0} values determined
130 for Ess75, Ess83, Ess96, Ess104, Ess112 and Mol are 2.20, 2.27, 2.40, 2.48, 2.56 and
131 2.23 MPa, respectively. For a reason of convenience, σ'_{v0} in both low pressure and high
132 pressure oedometers was set at 2.40 MPa for all tests.

133 4. Experimental results

134 4.1. Compressibility behavior

135 Figure 3 presents the loading-unloading-reloading stages and the corresponding changes in
136 vertical displacement in test Ess75Oedo1. Before the re-saturation phase, a loading from
137 0.125 to 2.4 MPa was applied to reach the in situ stress state. The soil sample was then
138 re-saturated using synthetic water. The subsequent unloading-reloading stages were as follows:
139 unloading from point A (2.4 MPa) to B (0.125 MPa); loading to C (16 MPa); unloading to D
140 (0.125 MPa); loading to E (32 MPa) and unloading to F (0.125 MPa). Common results were
141 obtained in terms of vertical displacements, *i.e.* compression upon loading and rebounding
142 upon unloading. Note that the French standards – AFNOR (1995, 2005) were applied as
143 regards the deformation stabilization for all odometer tests: stabilization is achieved when the
144 displacement rate is lower than 0.01mm/h.

145 Figure 4 presents the compression curve (void ratio versus $\log \sigma'_v$) of test Ess75Oedo1,
146 together with the compression curve of test Ess75Oedo2 in low pressure odometer. In test
147 Ess75Oedo2, after the re-saturation using synthetic water under 2.4 MPa stress, unloading
148 was performed from point I (2.4 MPa) to point II (0.05 MPa), then loading to point III
149 (3.2 MPa) and finally unloading to point IV (0.05 MPa).

150 The low pressure odometer test Ess75Oedo2 shows a quasi elastic behavior with narrow
151 unloading-loading loops. A deeper examination shows, however, that the reloading curve from
152 II to III is not linear in the plane e - $\log \sigma'_v$. This non-linearity can be also observed on the
153 curve of test Ess75Oedo1 on the reloading paths from B to C and from D to E. Note that the
154 results from the tests on other cores are similar to that shown in Figure 4. Obviously, it is
155 difficult to determine the pre-yield stress σ'_y using the Casagrande method on these curves. In
156 addition, this pre-yield stress, if any, does not correspond to the pre-consolidation pressure σ'_c
157 (σ'_y is much lower than σ'_c): σ'_c is equal to 2.4 MPa at point A, but when reloading from B to
158 C, σ'_y seems to be much lower, about 1 MPa. For this reason, in the following analysis only
159 σ'_c is used and its determination is based on the stress history: σ'_c is the maximum stress
160 applied in the odometer tests. For instance, $\sigma'_c = 16$ MPa for the paths C->D and D->E; σ'_c
161 = 32 MPa for the path E->F; $\sigma'_c = 3.2$ MPa for the path III->IV is 3.2 MPa.

162 Since the e - $\log \sigma'_v$ curves of Boom clay are not linear during unloading and unloading,
163 especially for the low pressure odometer tests, it is difficult to use an unique compression
164 index (C_c) and swell index (C_s) to describe the compression and swelling behavior. Hence the
165 above two indexes are determined stage by stage, and renamed C_c^* and C_s^* , respectively. It
166 should be pointed out that if the e - $\log \sigma'_v$ curves for the three stages (*i.e.* before pre-yielding,
167 after pre-yielding and unloading) are linear, the C_c^* becomes the same as C_c and C_s^* becomes
168 the same as C_s .

169 For the determination of secondary deformation coefficient C_{α} , standard method is used

170 based on the $e - \Delta \log t$ plot. The determination of C_c^* , C_s^* and C_α is illustrated in Figure 5.
171 Note that $C_\alpha = \Delta e / \Delta \log t$ is negative when loading and positive when unloading.

172 173 **4.2. Relation between C_α and σ'_v / σ'_c**

174 Figure 6 shows the variation of C_α versus the stress ratio σ'_v / σ'_c for all the six cores,
175 identified by both low pressure and high pressure oedometer tests. It appears that during
176 loading stage C_α ranges mostly from 0 to 0.01 especially when the vertical effective stress is
177 lower than the pre-consolidation stress. Some points beyond 0.01 can be observed when the
178 stress ratio is greater than 2. For core Ess112, C_α is very small and close to zero when the
179 stress ratio is less than 1. For the unloading stages, C_α ranges mostly from 0 to -0.01 for all
180 tests when the stress ratio is greater than 0.1. On the contrary, when the stress ratio is less than
181 0.1, C_α is less than -0.01. These observations lead to conclude that more significant secondary
182 consolidation takes place at higher stress ratios ($\sigma'_v / \sigma'_c > 1$) upon loading and more
183 significant secondary swelling takes place at lower stress ratios ($\sigma'_v / \sigma'_c < 0.1$).

184 Except the results of core Ess112 during loading, all other results show that C_α increases
185 almost linearly with the stress ratio in the semi-logarithmic plane, for both loading and
186 unloading stages. This is different from the results reported by other authors (Walker, 1969;
187 Brook and Mark, 2000; Yilmaz and Saglamer, 2007; You, 1999; Zhu *et al.*, 2005; Shriako *et*
188 *al.*, 2006; Suneel *et al.*, 2008; Costa and Ioannis, 2009) who observed that the relation
189 between C_α and $\log \sigma'_v / \sigma'_c$ during loading is rather convex.

190 191 **4.3. Relation between C_c^* or C_s^* and C_α**

192 Figure 7 shows the variations of C_α with C_c^* and C_s^* for all the cores. It appears that C_α
193 increases linearly with C_c^* , with a slope ranging from 0.019 to 0.029. Moreover, this linear
194 relation is independent of the state of consolidation: for a given core, all the points below and
195 beyond σ'_c are on the same line.

196 Mesri *et al.* (1994) analyzed the secondary consolidation behaviour of many soils, and
197 gave the correlation between the secondary consolidation coefficient (C_α) and the
198 compression index C_c as shown in Table 1. From the results obtained on Boom clay, it
199 appears that the ratio C_α / C_c^* falls in a narrow range from 0.019 to 0.029. In order to have a
200 mean value, all the results during loading are gathered in Figure 8, in terms of variations of
201 C_α versus C_c^* . A value of 0.024 is identified for the ratio C_α / C_c^* . Based on the classification
202 criterion in Table 1, one can conclude that Boom clay falls in the zone of shake and mudstone
203 whose C_α / C_c^* value ranges from 0.02 to 0.04.

204 Figure 7 also shows that during unloading, a bi-linear relation between C_α and C_s^* can be
205 observed: the turning point at a C_s^* value around 0.1. This turning point can be considered as
206 an indicator of changes from mechanical dominance to physical-chemical dominance in terms
207 of volume changes: when C_s^* is less than the value at the turning point, the clay shows a
208 mechanically dominated rebounding; by contrast, when C_s^* is larger than the value at the
209 turning point, the clay shows a physico-chemically dominated swelling. This particular
210 behaviour during unloading was also observed in other works: Delage *et al.* (2007) and Le *et*
211 *al.* (2011) conducted compression tests on unsaturated Boom clay with suction monitoring,
212 and observed that during unloading the soil suction increased slowly in the beginning and
213 then rapidly when the vertical stress decreased down to a threshold value; Cui *et al.* (2002)

214 observed that the microstructure of a compacted bentonite/sand mixture started to change
215 much more drastically when the suction was lower than 1 MPa; Cui *et al.* (2008) and Ye *et al.*
216 (2009) observed that the unsaturated hydraulic behaviour of compacted bentonite-based
217 materials under confined conditions changed drastically when the suction was lower than a
218 threshold value.

219 All the data of C_α versus C_s^* are gathered in Figure 9. In spite of the significant scatter, a
220 bilinear relation can be still identified, with -0.024 and -0.26 as slopes. It is interesting to note
221 that the absolute value of the slope of the first part (where the volume change behavior is
222 supposed to be governed by the mechanical effect) is equal to the value of C_α/C_c^* during
223 loading (0.024). This observation confirms that the first part of unloading ($C_s^* < 0.1$) gives
224 rise to a mechanically dominated rebounding, because the volume change behavior during
225 loading can be regarded as governed by the mechanical effects. The larger slope of the second
226 part (0.26, when $C_s^* > 0.1$) indicates a significant secondary swelling behavior compared to
227 the mechanical secondary consolidation behavior.

228

229 5. Conclusion

230 Both low pressure and high pressure oedometer tests were carried out with loading and
231 unloading on Boom clay samples taken by coring from Essen and Mol sites. The e -log σ'_v and
232 e -log t curves were plotted to determine the compression index C_c^* , swell index C_s^* and
233 secondary deformation coefficient C_α . Note that C_α was determined for either loading stages
234 (secondary consolidation) or unloading stages (secondary swelling). Different relations such
235 as $C_\alpha - \sigma'_v/\sigma'_c$, $C_\alpha - C_c^*$, and $C_\alpha - C_s^*$ were analyzed. The following conclusions can be
236 drawn:

- 237 (i) C_α increases almost linearly with the stress ratio σ'_v/σ'_c in the semi-logarithmic plane, for
238 both loading and unloading stages. This linear relation during loading was different from
239 that observed by other researchers who concluded rather a convex relation for other soils.
- 240 (ii) C_α increases linearly with C_c^* , with a slope of 0.024. In addition, this linear relation is
241 independent of the state of consolidation. During unloading, a bi-linear relation between
242 C_α and C_s^* was identified, with the turning point at a C_s^* value around 0.1 and the values
243 of slopes of -0.024 and -0.26, respectively.
- 244 (iii) The two slopes of the $C_\alpha - C_s^*$ curve relate to two different mechanisms: the first part
245 ($C_s^* < 0.1$) relates to a mechanically dominated rebounding whilst the second part ($C_s^* >$
246 0.1) relates to a physico-chemically dominated swelling. This observation was confirmed
247 by the equality of the slopes for the first unloading part and the loading part (0.024),
248 because the volume change behavior during loading can be regarded as governed by the
249 mechanical effects.
- 250 (iv) According to the classification criterion defined by Mesri *et al.* (1994), Boom clay falls in
251 the zone of shake or mudstone whose C_α/C_c^* value ranges from 0.02 to 0.04.

252

253 Acknowledgements

254 ONDRAF/NIRAS (The Belgian Agency for Radioactive Waste and Enriched Fissile Materials)

255 is greatly acknowledged for its financial support. The first author is grateful to the National
256 Science Foundation of China for its support (No 50908049).
257

258 **References:**

- 259 Abdullah, W.S., Al-Zoubi, M.S. and Alshibli, K.A. 1997. On the physicochemical aspects of
260 compacted clay compressibility. *Canadian Geotechnical Journal* 34, 551–559.
- 261 AFNOR, 1995. Sols : reconnaissance et essais: essai de gonflement à l'oedomètre,
262 détermination des déformations par chargement de plusieurs éprouvettes. XP P 94-091.
- 263 AFNOR, 2005. Geotechnical investigating and testing, Laboratory testing of soils, Part 5:
264 Incremental loading odometer test. XP CEN ISO/TS 17892-5.
- 265 Al-Shamrani, M., 1998. Application of the C_{α}/C_c concept to secondary compression of
266 Sabkha soils. *Canadian Geotechnical Journal* 35, 15-26.
- 267 Brook, E. and Mark A. A. 2000. Secondary compression of soft clay from Ballina. Proc.
268 GeoEng 2000, Melbourne, Australia.
- 269 Costas, A.A. and Ioannis, N.G. 2009. A new model for the prediction of secondary
270 consolidation index of low and medium plasticity clay soils. *European Journal of*
271 *Scientific Research* 34(4), 542-549.
- 272 Cui, Y.J., Loiseau, C. and Delage, P. 2002. Microstructure changes of a confined swelling soil
273 due to suction controlled hydration. Proc. of the Third Inter. Conf. on Unsaturated Soils
274 UNSAT2002, Recife, vol. 2, 593-598.
- 275 Cui, Y.J., Tang, A.M., Loiseau, C. and Delage, P. 2008. Determining the unsaturated
276 hydraulic conductivity of a compacted sand-bentonite under constant-volume and
277 free-swell conditions. *Physics and Chemistry of the Earth* 33, S462-S471.
- 278 Cui, Y.J., Le, T.T., Tang, A.M., Delage, P., and Li, X.L. 2009. Investigating the time
279 dependent behavior of Boom clay under thermomechanical loading. *Géotechnique* 59(4),
280 319-329.
- 281 De Craen, M., Wemaere, I., Labat, S., and Van Geet, M. 2006. Geochemical analyses of Boom
282 Clay pore water and underlying aquifers in the Essen-1 borehole. External report,
283 SCK.CEN-ER-19, 06/MDC/P-47, Belgium
- 284 Delage, P., Le, T.T., Tang, A.M., Cui, Y.J., and Li, X.L. 2007. Suction effects in deep Boom
285 clay samples. *Géotechnique* 57(2), 239-244.
- 286 Feng, T.W., Lee, J.Y. and Lee, Y.J. 2001. Consolidation behavior of a soft mud treated with
287 small cement content, *Engineering Geology* 59, 327-335.
- 288 Feng, Z.G., and Zhu, J.G. 2009. Experimental study on secondary behavior of soft clays.
289 *Journal of Hydraulic Engineering* 40(5), 583-588 (In Chinese).
- 290 Le, T.T., Cui, Y.J., Munoz, J.J., Delage, P. and Li, X.L. 2011. Studying the hydraulic and
291 mechanical coupling in Boom clay using an oedometer equipped with a high capacity
292 tensiometer. *Frontier of Architecture and Civil Engineering in China* 5(2), 160-170.
- 293 Mesri, G., and Castro, A. 1987. The C_{α}/C_c concept and K_o during secondary compression.
294 *Journal of Geotechnical Engineering Division* 112(3), 230-247.
- 295 Mesri, G., Kwan, L.D.O., and Feng, W.T. 1994. Settlement of embankment on soft clays. Proc.
296 Of settlement 94, ASCE GSP 40, 8-56.
- 297 Mesri, G., Stark, T. D., Ajlouni, M. A., and Chen, C. S. 1997. Secondary compression of peat
298 with or without surcharging. *Journal of the Geotechnical Engineering Division* 123(5),
299 411-421.
- 300 Mesri, G., 2004. Primary compression and secondary compression, Proc. of Soil Behavior and
301 Soft Ground Construction, ASCE GSP 119, 122-166.

302 Mesri, G. and Vardhanabhuti, B. 2009. Compression of granular materials. *Canadian*
303 *Geotechnical Journal* 46, 369–392.

304 Shriako, H., Sugiyama, M., Tonosaki, A. and Akaishi, M. 2006. Secondary compression
305 behavior in standard consolidation tests. *Proc. of Schl. Eng, Tokai University* 31, 27-32

306 Suneel, M., Park, L.K., and Chulim J. 2008. Compressibility characteristics of Korean marine
307 clay. *Marine Georesources and Geotechnology* 26, 111–127.

308 Tan, Z.H., 2002. The behavior of compression and consolidation for clays. These of Taiwan
309 Central University, China, 428 pp. (In Chinese).

310 Walker, L.K. and Raymond, G.P. 1968. The prediction of consolidation rates in a cemented
311 clay. *Canadian Geotechnical Journal* 5(4), 192-216.

312 Walker, L.K., 1969. Secondary settlement in sensitive clays. *Canadian Geotechnical Journal*
313 6(2), 219-222.

314 Ye, W.M., Cui, Y.J., Qian, L.X., Chen, B. 2009. An experimental study of the water transfer
315 through compacted GMZ bentonite. *Engineering Geology* 108, 169 – 176.

316 Yilmaz, E. and Saglamer A. 2007. Evaluation of secondary compressibility of a soft clay. *The*
317 *bulletin of the Istanbul Technical University* 54 (1), 7-13.

318 You, M.Q., 1999. Compression and consolidation behavior under different sampling, loading
319 methods. Thesis of Taiwan Central University, China, 124 pp. (In Chinese).

320 Zhang, J.H., Miao, L.C. and Huang, X.M. 2005. Study on secondary consolidation
321 deformation of soft clay. *Journal of Hydraulic Engineering* 36(1), 1-5 (In Chinese).

322 Zhu, H.H, Chen, X.P., Zhang F.J. and Huang, L.J. 2005. Consolidation behaviors of soft soil
323 in Nansha, *Geotechnical Investigation and Surveying* 33(1), 1-3 (In Chinese).

324 **List of Tables**

325 Table 1. Soil classification according to the values C_α/C_c (Mesri *et al.*, 1994)

326 Table 2. Geotechnical properties of the soil cores studied

327 **List of Figures**

328 Figure 1. Locations of the sampling sites (De Craen *et al.*, 2006)

329 Figure 2 Sketch of high pressure oedometer

330 Figure 3. Vertical effective stress and displacement versus elapsed time (Ess75Oedo1)

331 Figure 4. Compression curves from oedometer tests (Ess75Oedo1 and Ess75Oedo2)

332 Figure 5. Determination of parameters C_c^* , C_s^* and C_α

333 Figure 6. C_α versus stress ratio σ'_v/σ'_c . (a) Core Ess75; (b) Core Ess83; (c) Core Ess96; (d) Core
334 Ess104; (e) Core 112; (f) Core Mol

335 Figure 7. C_α versus C_c^* and C_s^* . (a) Core Ess75; (b) Core Ess83; (c) Core Ess96; (d) Core Ess104; (e)
336 Core 112; (f) Core Mol

337 Figure 8. C_α versus C_c^*

338 Figure 9. C_α versus C_s^*

339

340

341 Table 1. Soil classification according to the values C_d/C_c (Mesri *et al.*, 1994)

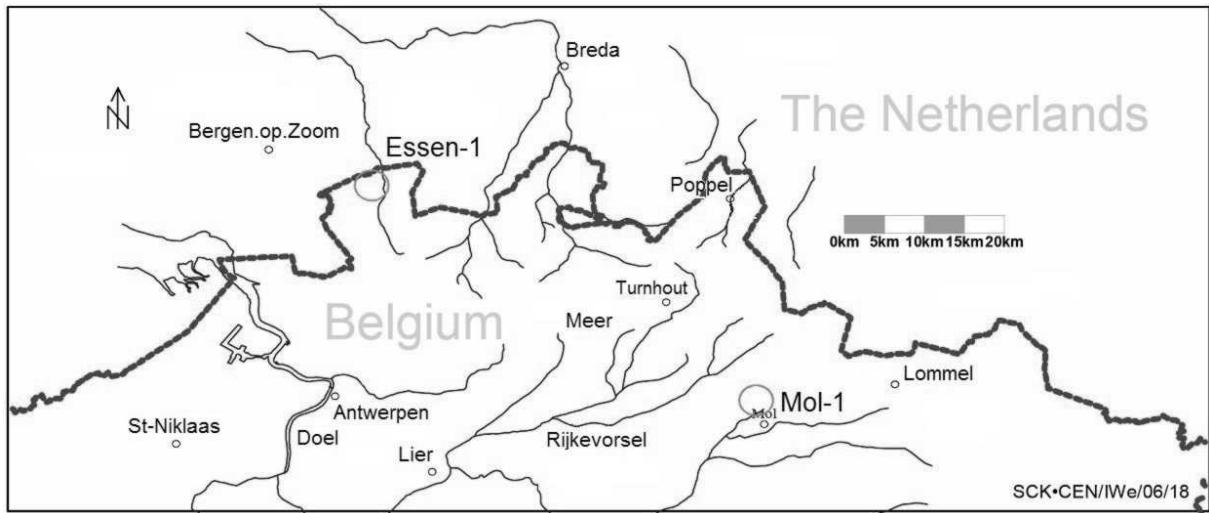
Material	C_d/C_c
Granular soils including rockfill	$C_d/C_c = 0.02 \pm 0.01$
Shake and mudstone	$C_d/C_c = 0.03 \pm 0.01$
Inorganic clays and silts	$C_d/C_c = 0.04 \pm 0.01$
Organic clays and silts	$C_d/C_c = 0.05 \pm 0.01$
Peat and muskeg	$C_d/C_c = 0.06 \pm 0.01$

342

343

344 Table 2. Geotechnical properties of the soil cores studied

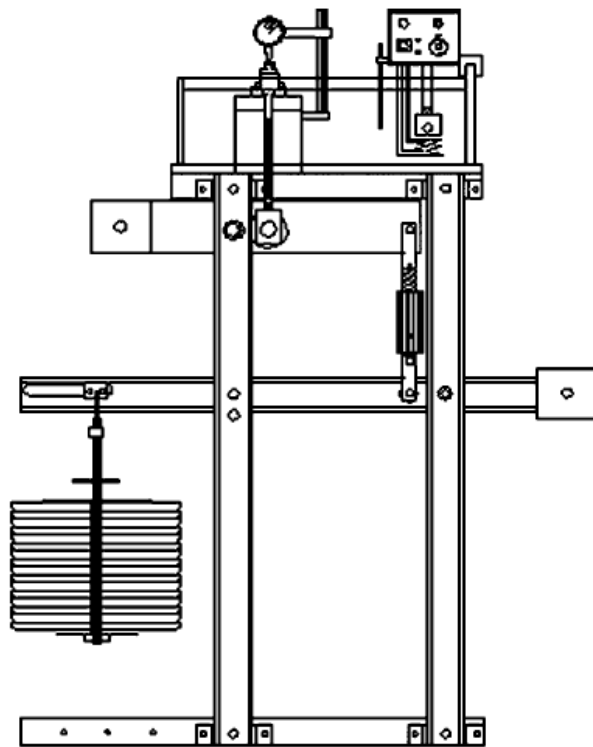
Core	Depth (m)	Member	ρ_s (Mg/m ³)	w_L (%)	w_p (%)	I_p (%)	w_0 (%)	e_0
Ess75	218.91-219.91	Putte	2.65	78	33	45	29.7	0.785
Ess83	226.65-227.65	Putte	2.64	70	33	37	27.2	0.730
Ess96	239.62-240.62	Terhagen	2.68	69	33	36	26.5	0.715
Ess104	247.90-248.91	Terhagen	2.68	68	29	39	27.7	0.700
Ess112	255.92-256.93	Terhagen	2.67	62	25	37	27.3	0.755
Mol	223	Putte	2.67	68	26	42	23.6	0.625



345
346

Figure 1. Locations of the sampling sites (De Craen *et al.*, 2006)

347



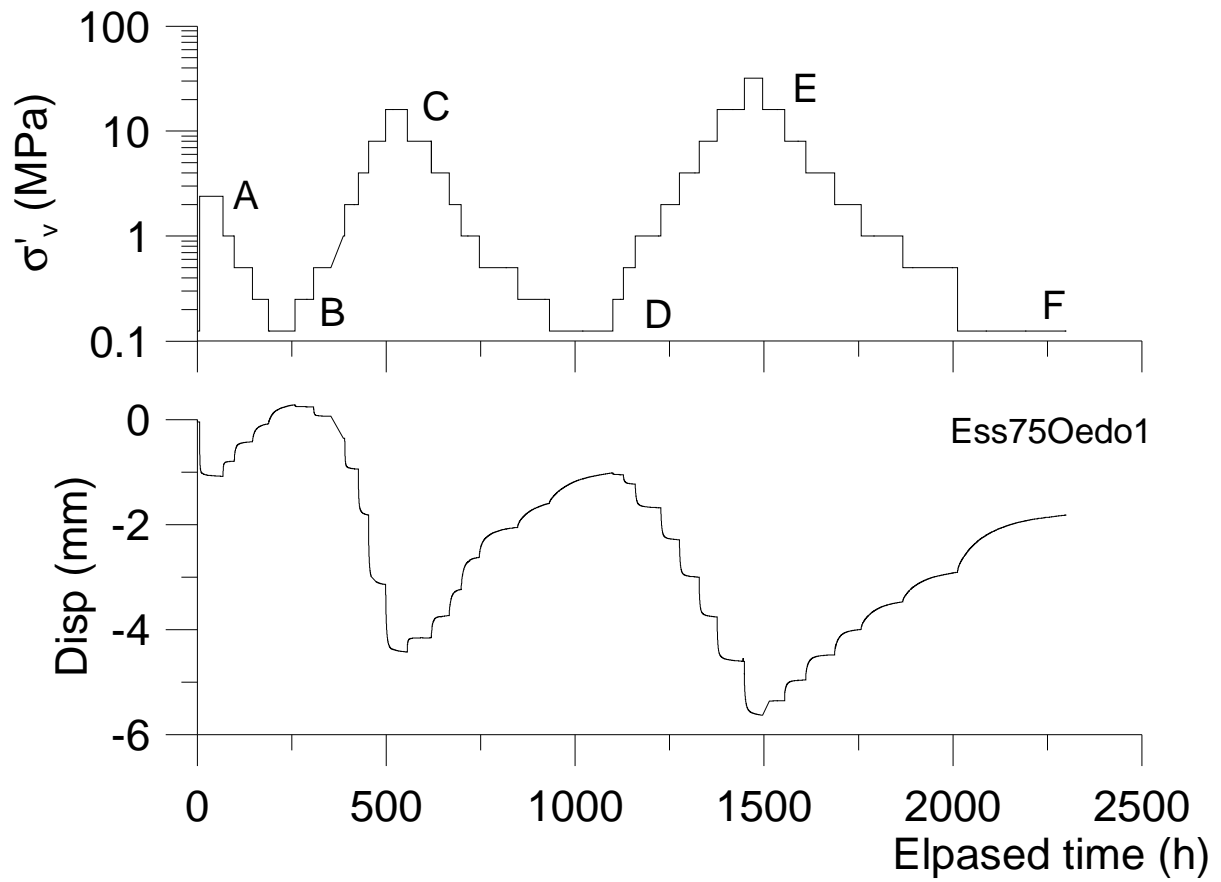
348

349

350

Figure 2 Sketch of high pressure oedometer

351

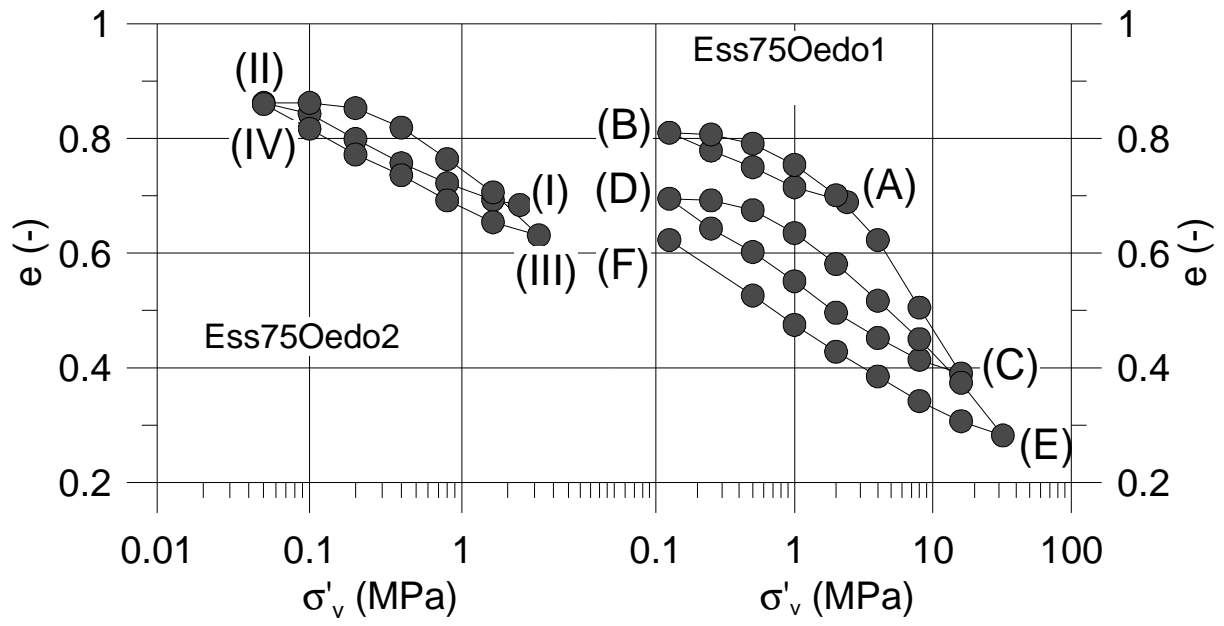


352

353

Figure 3. Vertical effective stress and displacement versus elapsed time (Ess75Oedo1)

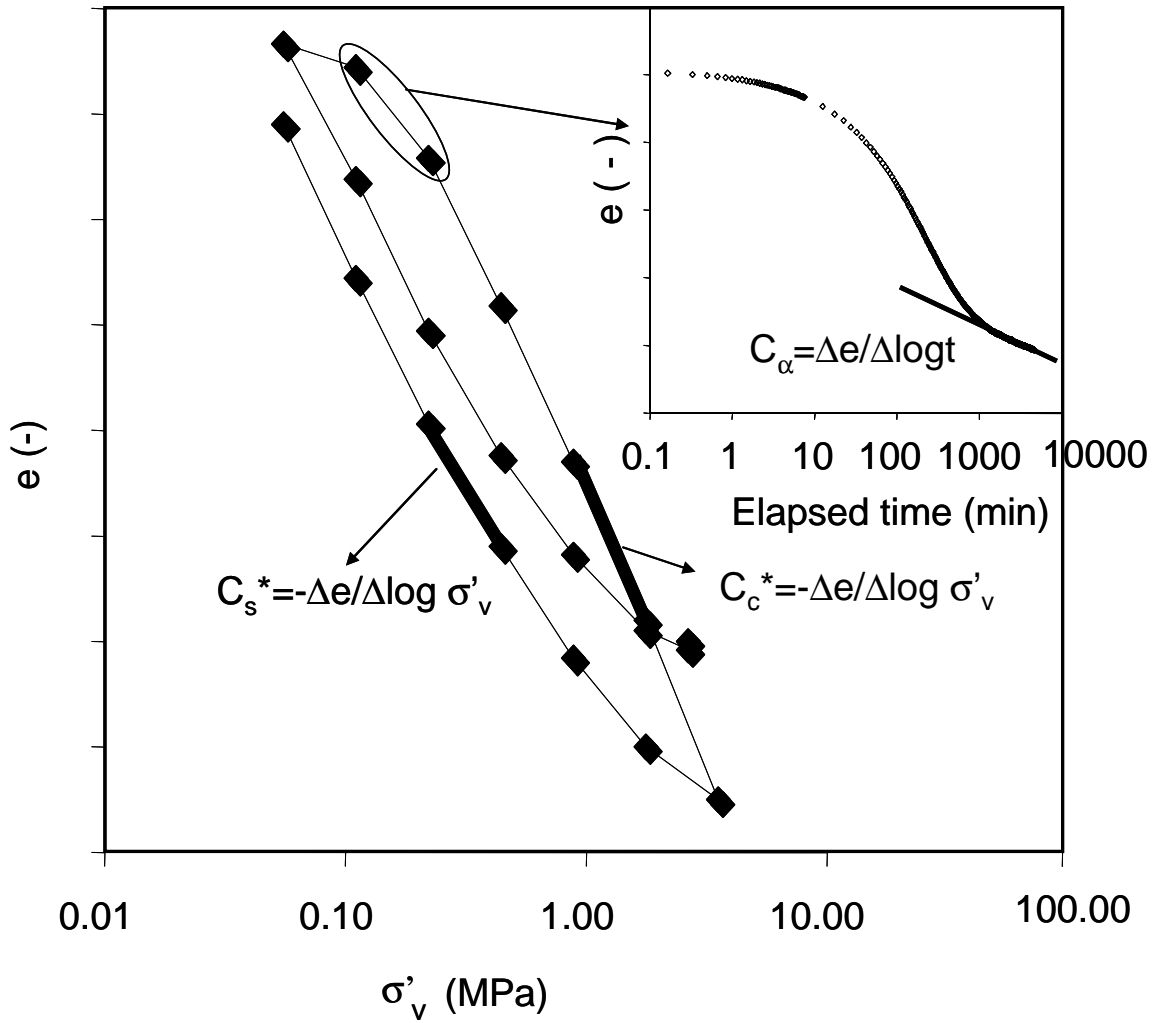
354



355

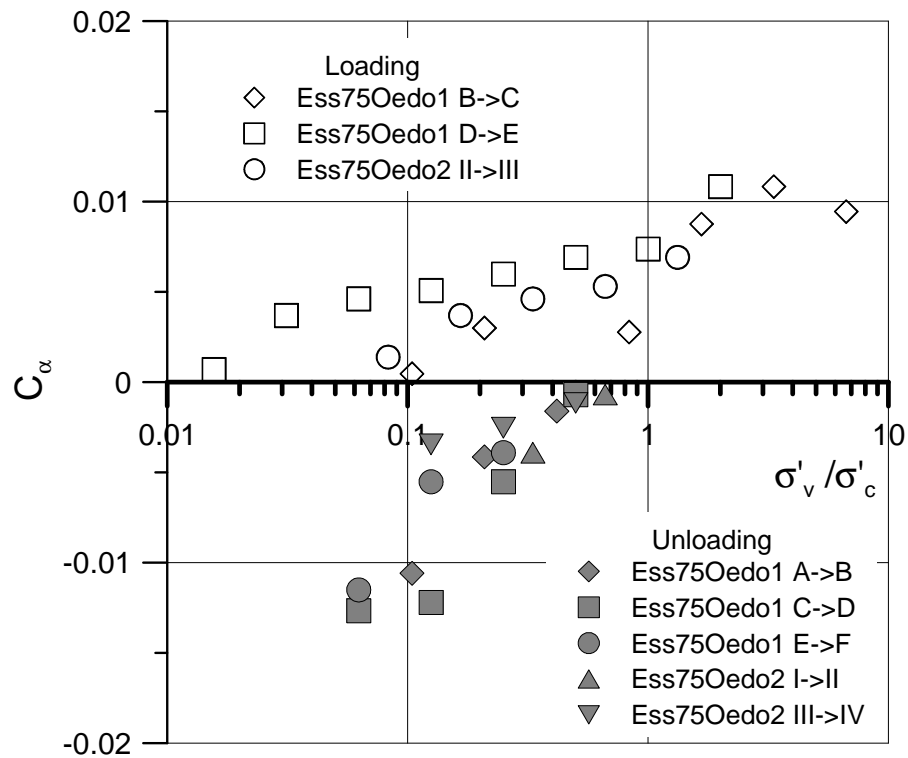
356

Figure 4. Compression curves from oedometer tests (Ess75Oedo1 and Ess75Oedo2)

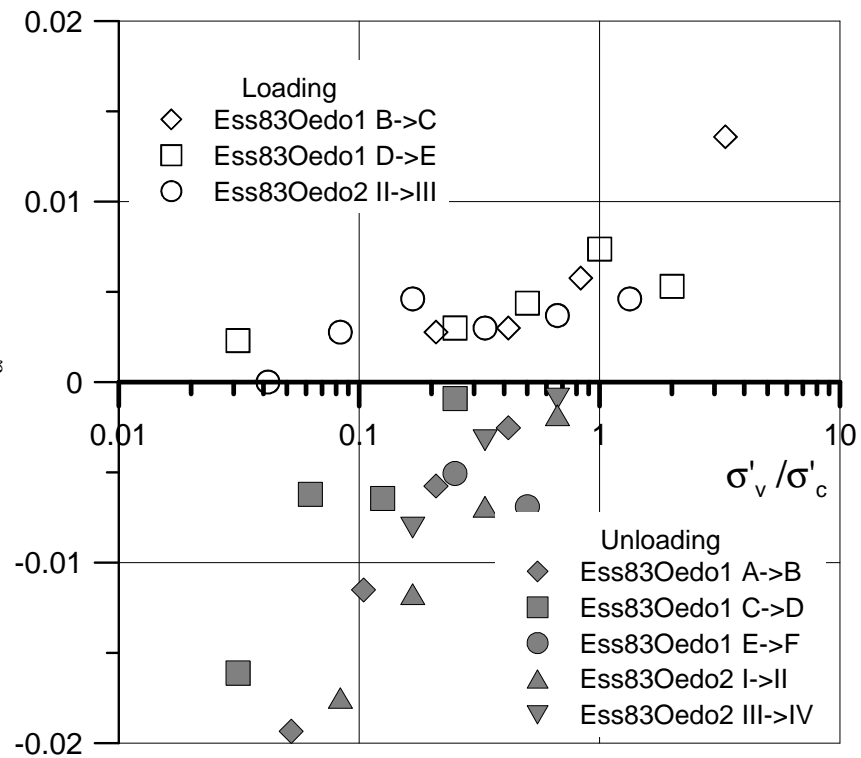


358
359

Figure 5. Determination of parameters C_c^* , C_s^* and C_α

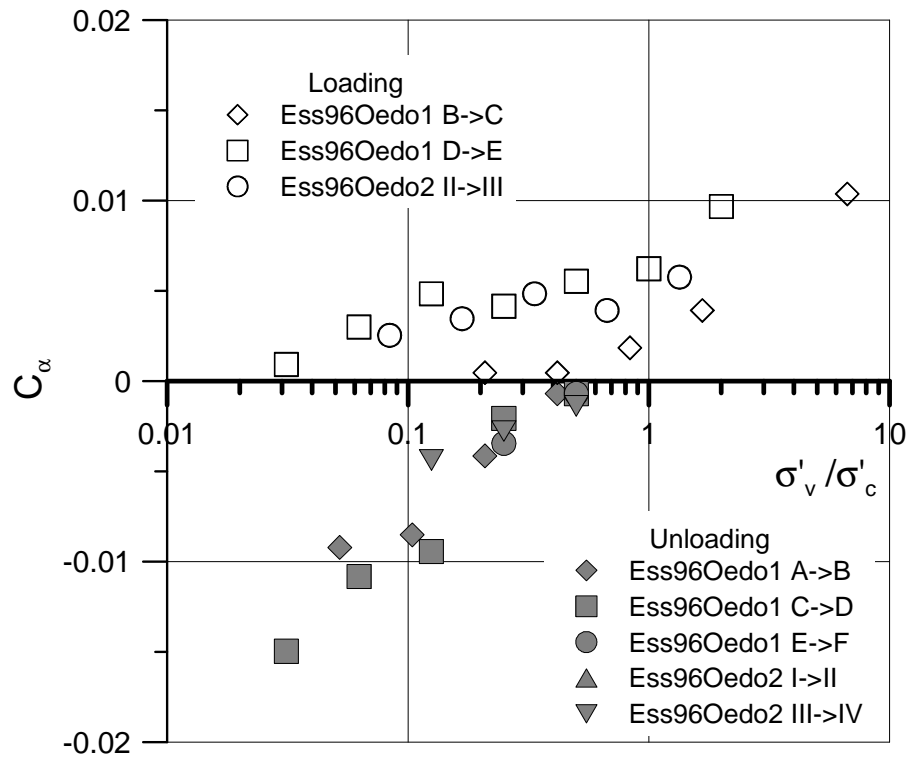


(a)

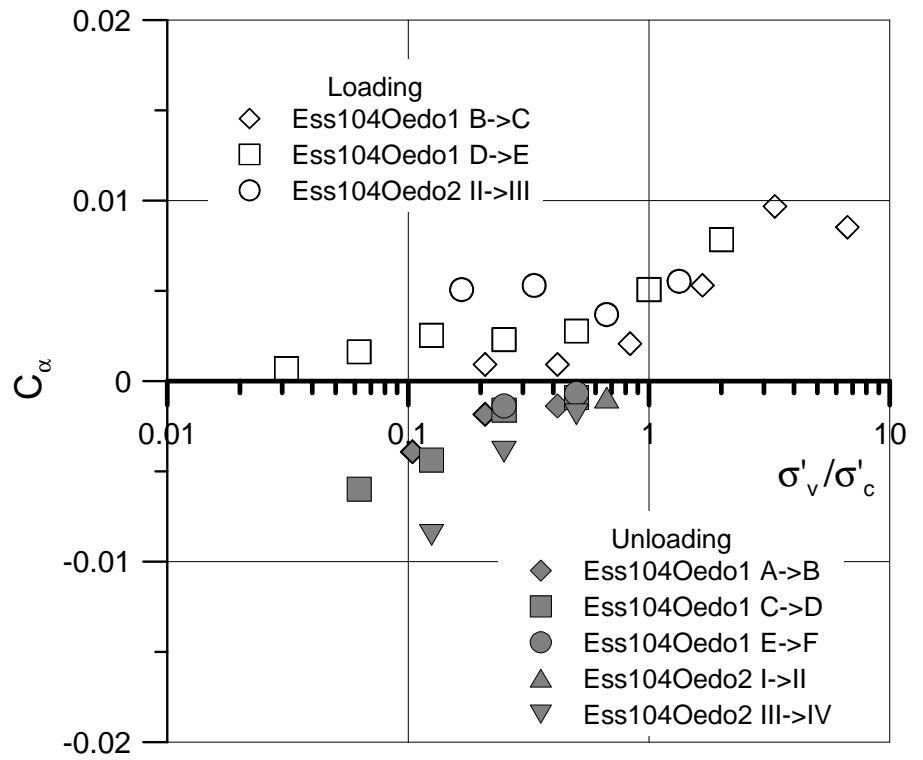


(b)

360
361



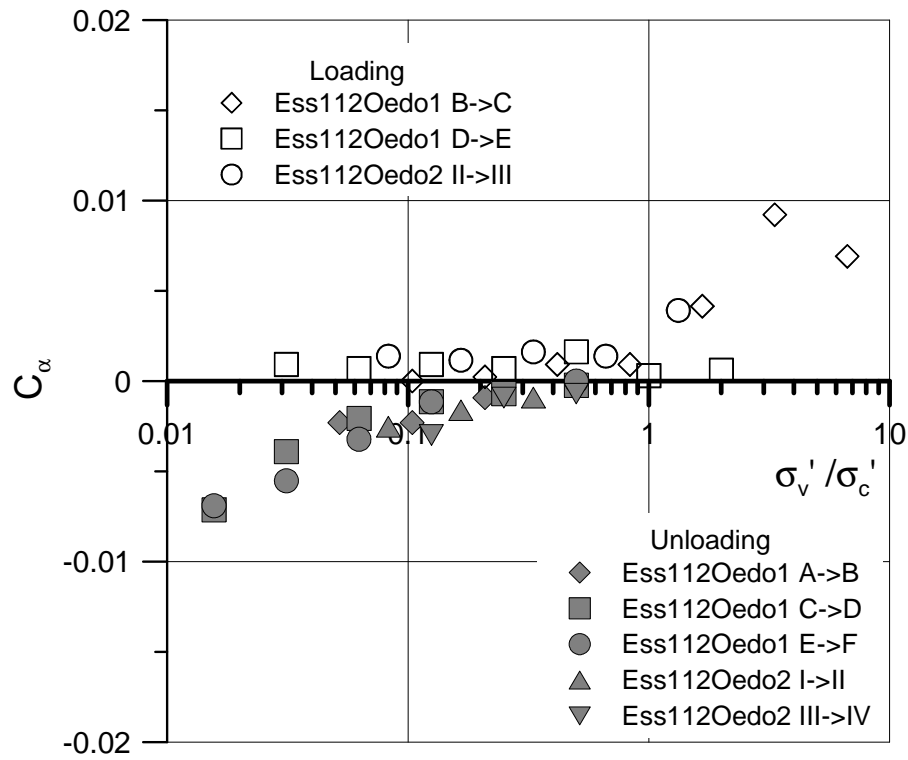
(c)



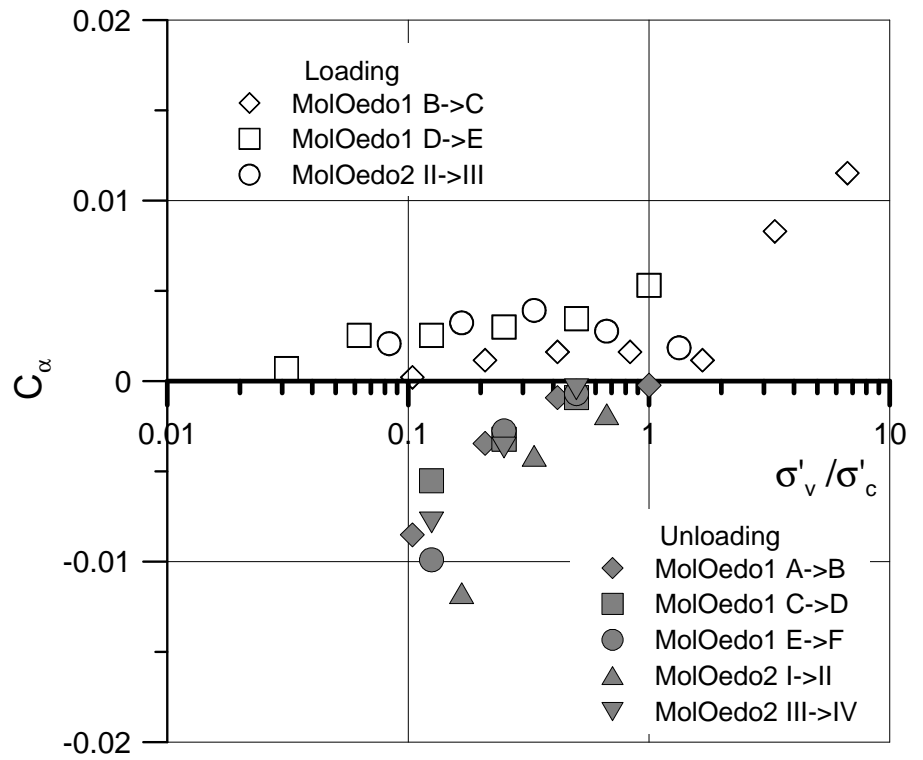
(d)

362

363



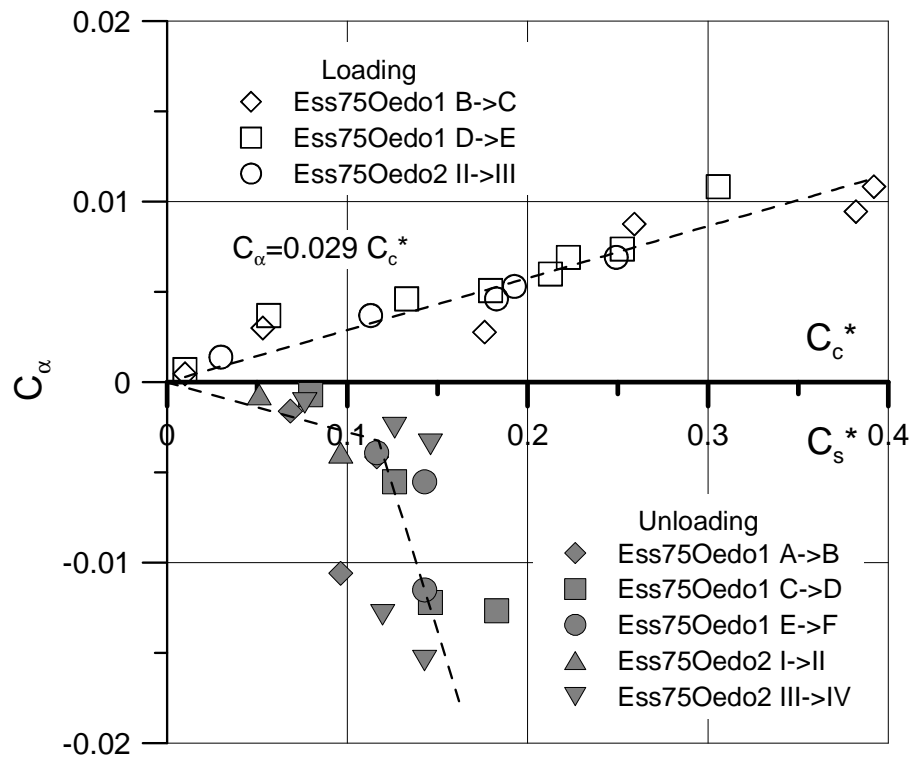
(e)



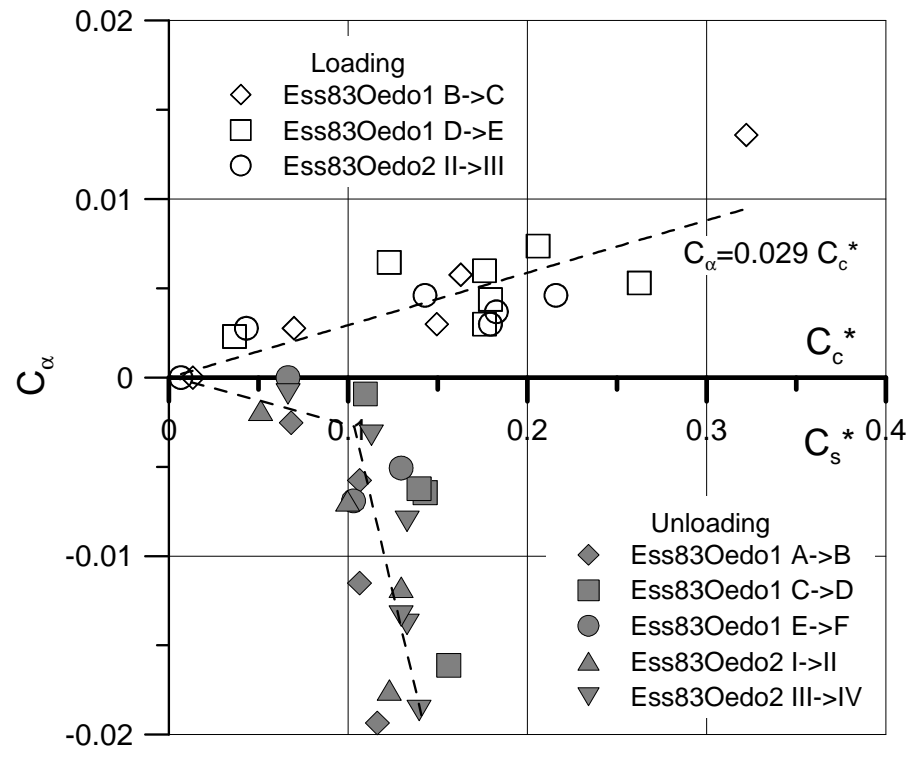
(f)

Figure 6. C_α versus stress ratio σ'_v/σ'_c . (a) Core Ess75; (b) Core Ess83; (c) Core Ess96; (d) Core Ess104; (e) Core 112; (f) Core Mol

364
365
366
367



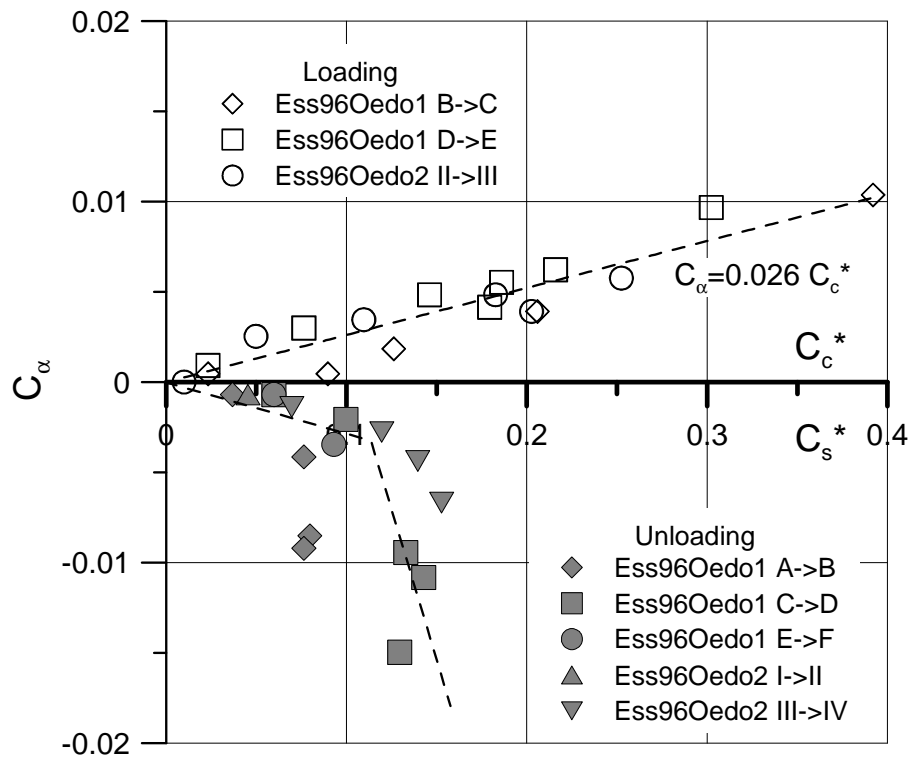
(a)



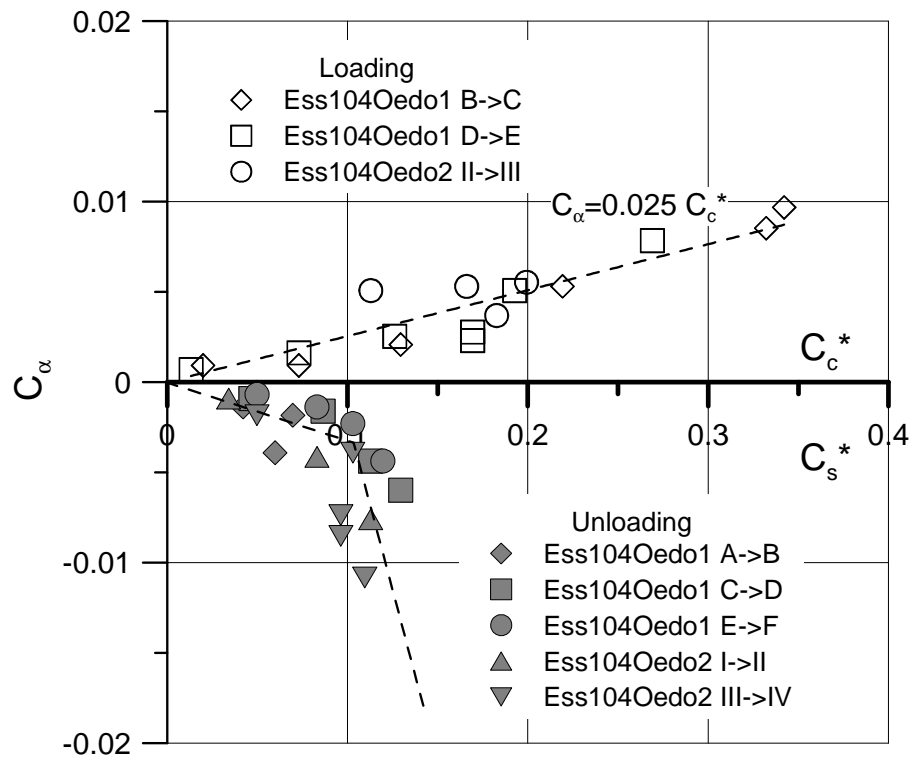
(b)

368

369



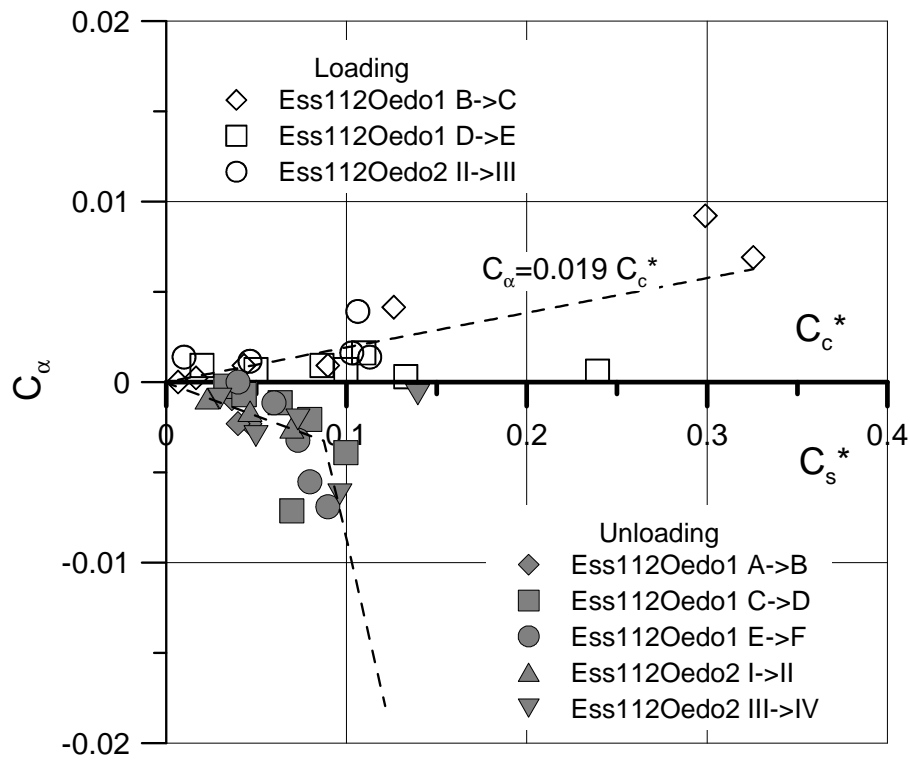
(c)



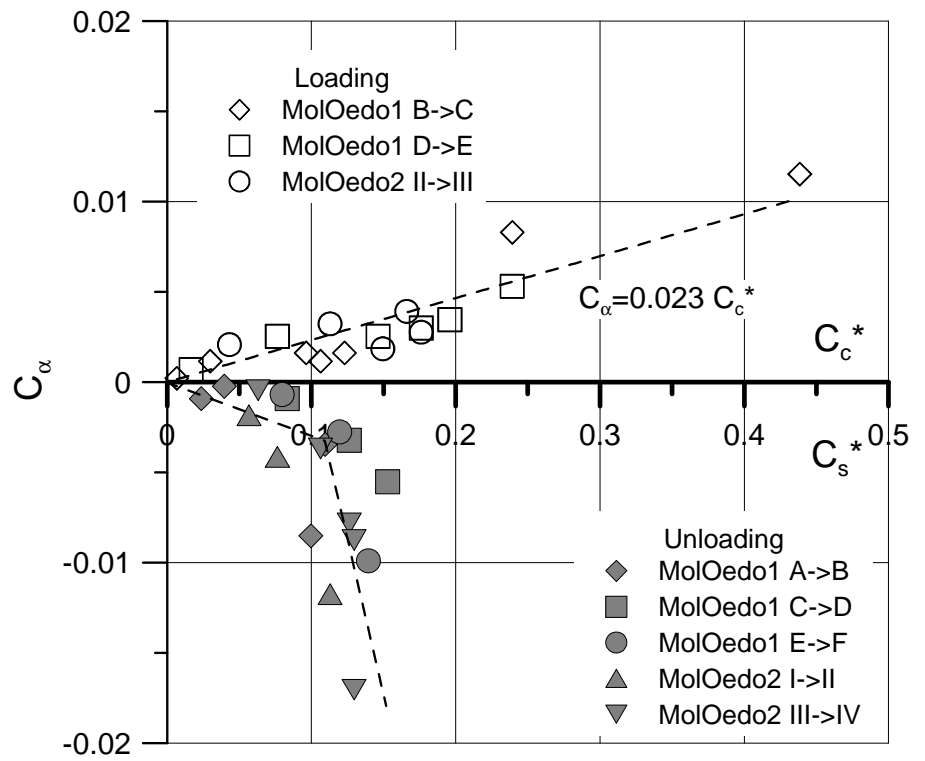
(d)

370

371



(e)

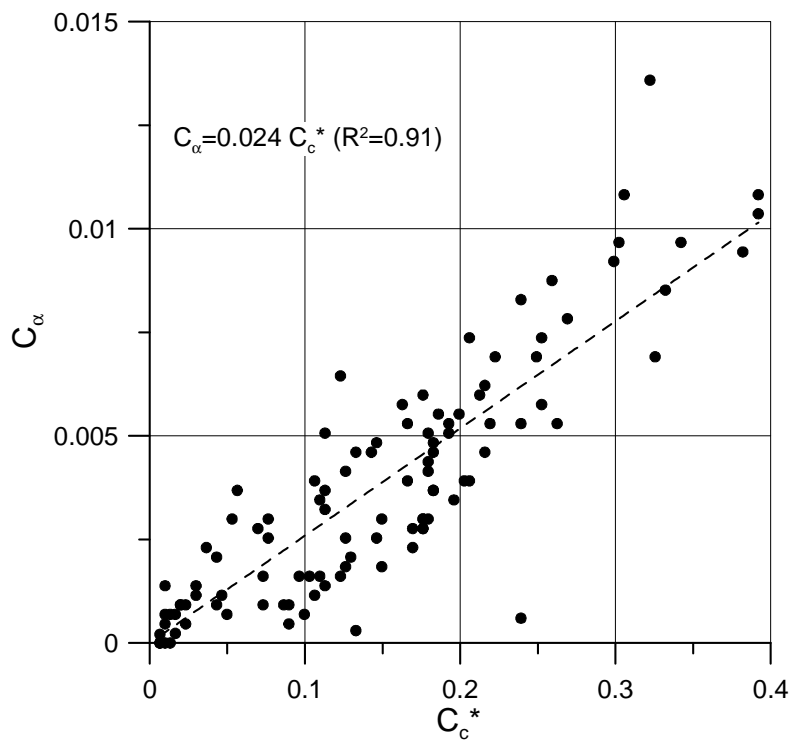


(f)

Figure 7. C_α versus C_c^* and C_s^* . (a) Core Ess75; (b) Core Ess83; (c) Core Ess96; (d) Core Ess104; (e) Core 112; (f) Core Mol

372
373
374
375

376

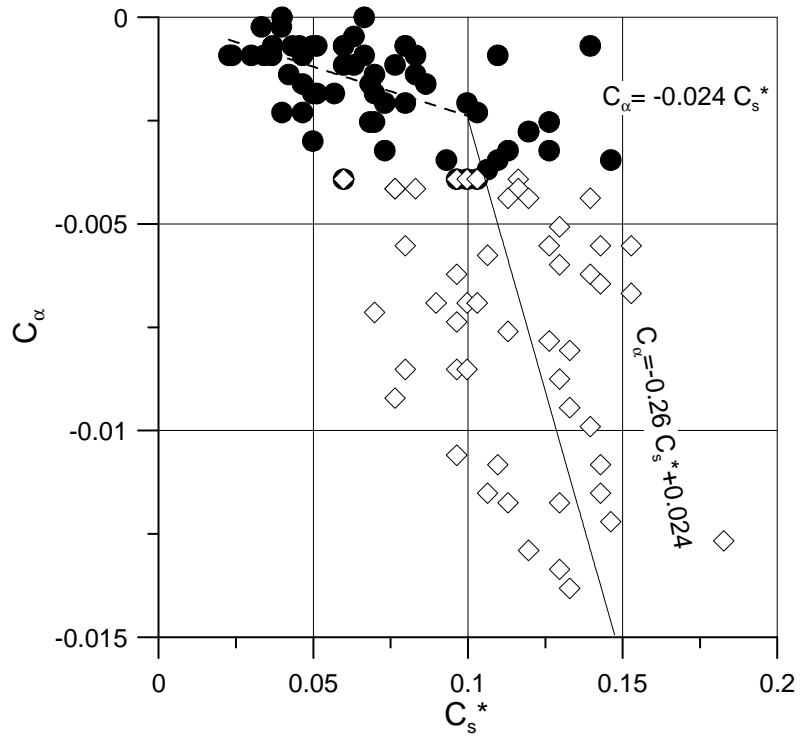


377

378

Figure 8. C_α versus C_c^*

379



380

381

Figure 9. C_α versus C_s^*